

1 **Rotavirus as an Expression Platform of the SARS-CoV-2 Spike Protein**

2

3 Asha A. Philip and John T. Patton*

4 Department of Biology, Indiana University, Bloomington, IN 47405, USA

5

6 ***Correspondence:** John T. Patton, Department of Biology, Indiana University, 212 S.

7 Hawthorne Drive, Simon Hall 011, Bloomington, IN 47405 USA

8

9 **Email addresses:** Asha A. Philip, aaphilip@iu.edu; John T. Patton, jtpatton@iu.edu

10

11 **Running Head:** Rotavirus expressing SARS-CoV-2 spike

12

13 **Word Counts:** Abstract (250), Text (3318)

14

15 **Abstract**

16 Rotavirus, a segmented double-stranded RNA virus, is a major cause of acute gastroenteritis in
17 young children. The introduction of live oral rotavirus vaccines has reduced the incidence of
18 rotavirus disease in many countries. To explore the possibility of establishing a combined
19 rotavirus-SARS-CoV-2 vaccine, we generated recombinant (r)SA11 rotaviruses with modified
20 segment 7 RNAs that contained coding sequences for NSP3 and FLAG-tagged portions of the
21 SARS-CoV-2 spike (S) protein. A 2A translational element was used to drive separate
22 expression of NSP3 and the S product. rSA11 viruses were recovered that encoded the S-protein
23 S1 fragment, N-terminal domain (NTD), receptor-binding domain (RBD), extended receptor-
24 binding domain (ExRBD), and S2 core (CR) domain (rSA11/NSP3-fS1, -fNTD, -fRBD, -
25 fExRBD, and -fCR, respectively). Generation of rSA11/fS1 required a foreign-sequence
26 insertion of 2.2-kbp, the largest such insertion yet made into the rotavirus genome. Based on
27 isopycnic centrifugation, rSA11 containing S sequences were denser than wildtype virus,
28 confirming the capacity of the rotavirus to accommodate larger genomes. Immunoblotting
29 showed that rSA11/-fNTD, -fRBD, -fExRBD, and -fCR viruses expressed S products of
30 expected size, with fExRBD expressed at highest levels. These rSA11 viruses were genetically
31 stable during serial passage. In contrast, rSA11/NSP3-fS1 failed to express its expected 80-kDa
32 fS1 product, for unexplained reasons. Moreover, rSA11/NSP3-fS1 was genetically unstable, with
33 variants lacking the S1 insertion appearing during serial passage. Nonetheless, these results
34 emphasize the potential usefulness of rotavirus vaccines as expression vectors of portions of the
35 SARS-CoV-2 S protein (e.g., NTD, RBD, ExRBD, and CR) with sizes smaller than the S1
36 fragment.

37 **Importance**

38 Among the vaccines administered to children in the US and many other countries are those
39 targeting rotavirus, a segmented double-stranded RNA virus that is a major cause of severe
40 gastroenteritis. In this study, we have examined the feasibility of modifying the rotavirus genome
41 by reverse genetics, such that the virus could serve as an expression vector of the SARS-CoV-2
42 spike protein. Results were obtained showing that recombinant rotaviruses can be generated that
43 express domains of the SARS CoV-2 spike protein, including the receptor-binding domain
44 (RBD), a common target of neutralizing antibodies produced in individuals infected by the virus.
45 Our findings raise the possibility of creating a combined rotavirus-COVID-19 vaccine that could
46 be used in place of current rotavirus vaccines.

47

48 **Key words.** rotavirus, rotavirus vaccine, reverse genetics, *Reoviridae*, expression vector, SARS-
49 CoV-2, COVID-19 vaccine, spike protein

50 INTRODUCTION

51 The impact of severe acute respiratory syndrome coronavirus 2 (SARS-CoV-2) on human
52 mortality and morbidity has stimulated broad ranging efforts to develop vaccines preventing
53 coronavirus disease 19 (COVID-19) (1,2). Given that the virus can cause asymptomatic and
54 symptomatic infections in individuals of all ages, including infants and young children,
55 comprehensive strategies to control the SARS-CoV-2 pandemic may require modification of
56 childhood immunization programs to include COVID-19 vaccines (3,4). Among the vaccines
57 routinely administered to infants in the US and many other countries, are those targeting
58 rotavirus, a segmented double-stranded RNA (dsRNA) virus that is a primary cause of severe
59 acute gastroenteritis (AGE) in children during the first 5 years of life (5). The most widely used
60 rotavirus vaccines are given orally and formulated from live attenuated virus strains (6). These
61 vaccines induce the production of neutralizing IgG and IgA antibodies (7,8,9) and have been
62 highly effective in reducing the incidence of rotavirus hospitalizations and mortality (10,11).

63 Advances in rotavirus reverse genetics technologies have allowed the generation of
64 recombinant rotaviruses that serve as expression platforms of heterologous proteins (12-19). The
65 rotavirus genome consists of 11 segments of dsRNA, with a total size of ~18.6 kbp for group A
66 strains (rotavirus species A) typically associated with pediatric AGE (20). Most of the genome
67 segments contain a single open-reading frame (ORF); these encode the 6 structural (VP1-VP4,
68 VP6-VP7) or 6 nonstructural (NSP) viral proteins (21). The recently-developed rotavirus reverse
69 genetics systems consist of eleven T7 transcription (pT7) vectors, each directing synthesis of a
70 unique viral (+)RNA when transfected into baby-hamster kidney cells producing T7 RNA
71 polymerase (BHK-T7 cells). In some cases, support plasmids expressing capping enzymes
72 [African swine fever virus NP868R (22) or vaccinia virus D1L/D12R (18)] or fusion proteins

73 [avian reovirus p10FAST (18)] are co-transfected with the pT7 vectors to enhance recovery of
74 recombinant viruses. Rotavirus reverse genetics systems have been used to mutate several of the
75 viral genome segments and to generate virus strains that express reporter proteins (13,17,23-26).

76 Genome segment 7 of group A rotaviruses encodes NSP3 (36 kDa), an RNA-binding
77 protein that acts a translation enhancer of viral (+)RNAs and is expressed at moderate levels in
78 infected cells (27,28). In a previous study, we showed that the single NSP3 ORF could be re-
79 engineered by reverse genetics to express two separate proteins through placement of a
80 teschovirus 2A translational stop-restart element at the end of the NSP3 ORF, followed by the
81 coding sequence for a heterologous protein (17). Through this approach, well-growing
82 genetically-stable recombinant rotaviruses have been generated that express NSP3 and one or
83 more fluorescent proteins (FPs) [e.g., mRuby (red), UnaG (green), TagBFP (blue), etc.] from
84 segment 7, an advance allowing study of rotavirus biology by live cell imaging (15). The NSP3
85 product of these recombinant viruses is functional, capable of dimerization and inducing the
86 nuclear accumulation of the cellular poly(A)-binding protein (16,17). Thus, recombinant
87 rotaviruses that express foreign proteins via addition of a 2A element and coding sequence into
88 segment 7 downstream of the NSP3 ORF retain the full complement of functional viral ORFs.

89 As a step towards developing a combined rotavirus-SARS-CoV-2 vaccine, we explored
90 the possibility of generating recombinant rotaviruses that express regions of the SARS-CoV-2
91 spike (S) protein through re-engineering of the NSP3 ORF in segment 7. Trimers of the S protein
92 form crown-like projections that emanate from the lipid envelop surrounding the SARS-CoV-2
93 virion (29,30). Cleavage of the trimeric spikes by extracellular furin-like proteases generates S1
94 and S2 fragments, each which possess activities essential for virus entry (Fig. 1). The S1
95 fragment includes an N-terminal domain (NTD) and a receptor-binding domain (RBD), the latter

96 mediating virus interaction with the cell surface receptor angiotensin-converting enzyme 2
97 (ACE2) (31). The S2 fragment is responsible for S-protein trimerization and contains fusion
98 domains that are essential for virus entry. SARS-CoV-2-specific antibodies with neutralizing
99 activity have been mapped to various regions of the S protein, including the NTD, RBD, and
100 fusion domains (32-35). We determined that by inserting S coding sequences into rotavirus
101 genome segment 7 downstream of the NSP3 ORF and a 2A element, well-growing genetically-
102 stable recombinant rotaviruses can be made that express all or portions of the S1 and S2
103 fragment. These findings raise the possibility of constructing rotavirus vaccine strains that are
104 not only capable of inducing immunological protective responses against rotavirus, but also
105 COVID-19.

106

107 **RESULTS AND DISCUSSION**

108 **Modified segment 7 (NSP3) expression vectors containing SARS-CoV-2 S sequences.**

109 To examine the possibility of using rotavirus as an expression platform for regions of the SARS-
110 CoV-2 S protein, we replaced the NSP3 ORF in the pT7/NSP3SA11 transcription vector with a
111 cassette comprised of the NSP3 ORF, a porcine teschovirus 2A element, and a coding sequence
112 of the S protein (Fig. 2). The cassette included a flexible GAG hinge between the coding
113 sequence for NSP3 and the 2A element and a 3x FLAG (f) tag between the coding sequences for
114 the 2A element and the S region. This approach was used to generate a set of vectors
115 (collectively referred to as pT7/NSP3-CoV2/S vectors) that contained coding sequences for
116 SARS-CoV-2 S1 (pT7/NSP3-2A-fS1), NTD (pT7/NSP3-2A-fNTD), RBD (pT7/NSP3-2A-
117 fRBD), an extended form of the RBD (ExRBD) (pT7/NSP3-2A-fExRBD), and the S2 core
118 region (CR) including its fusion domains (pT7/NSP3-2A-fCR) (Fig. 1). The S sequences were

119 inserted into the pT7/NSP3SA11 vector at the same site as used before in the production of
120 recombinant SA11 (rSA11) rotaviruses expressing FPs (15-17).

121 **Recovery of rSA11 rotaviruses with segment 7 dsRNA containing S sequences.** To
122 generate rSA11 viruses, BHK-T7 monolayers were transfected with a complete set of pT7/SA11
123 expression vectors, except pT7/NSP3SA11 was replaced with a pT7/NSP3-CoV2/S vector, and a
124 CMV expression plasmid (pCMV-NP868R) encoding the capping enzyme of African swine
125 fever virus. In transfection mixtures, plasmids encoding rotavirus NSP2 (pT7/NSP2SA11) and
126 NSP5 (pT7/NSP5SA11) were included at levels three-fold greater than the other pT7/SA11
127 vectors. BHK-T7 cells were overseeded with MA104 cells two days following transfection. The
128 BHK-T7/MA104 cell mixture was freeze-thawed three days later, and the rSA11 viruses were
129 recovered by plaque isolation and amplified by 1 or 2 cycles of growth in MA104 cells prior to
130 characterization (36). Properties of the rSA11 viruses are summarized in Table 1.

131 Based on gel electrophoresis, rSA11 viruses generated with pT7/NSP3-S vectors
132 (collectively referred to as rSA11/NSP3-CoV2/S viruses) contained segment 7 dsRNAs that
133 were much larger than that of wildtype rSA11 (rSA11/wt) virus (Fig. 3). Sequence analysis
134 confirmed that the segment 7 dsRNAs of the rSA11/NSP3-CoV2/S viruses matched the segment
135 7 sequences present in the pT7/NSP3-CoV2/S vectors (data not shown). The re-engineered
136 segment 7 dsRNA of virus isolate rSA11/NSP3-fS1 had a length of 3.3 kbp, accounting for its
137 electrophoretic migration near the largest rotavirus genome segment (segment 1), which is
138 likewise 3.3 kbp in length (Table 1, Fig. 3A). The segment 7 dsRNA of rSA11/NSP3-fS1
139 contains a 2.2-kbp foreign sequence insertion, the longest foreign sequence that has been
140 introduced into the segment 7 dsRNA, or for that matter, any rotavirus genome segment. The
141 previously longest 7 dsRNA engineered into rSA11 was the 2.4-kbp segment 7 dsRNA of

142 rSA11/NSP3-fmRuby-P2A-fUnaG, which contained a cassette that encoded three proteins
143 (NSP3, UnaG, mRuby) (17). The total genome size of rSA11/NSP3-fS1 is 20.8 kbp, 12% greater
144 than that of rSA11/wt (37). This is the largest genome known to exist within a rotavirus isolate
145 and demonstrates the capacity of rotavirus to replicate and package large amounts of foreign
146 sequence.

147 The segment 7 dsRNAs of virus isolates, rSA11/NSP3-fNTD, -fRBD, -fExRBD, and -
148 fCR, were determined to have lengths of 2.1, 1.8, 2.1, and 2.3 kbp, respectively (Table 1), and as
149 expected from their sizes, migrated on RNA gels between rotavirus genome segments 3 (2.6 kbp)
150 and 5 (1.6 kbp) (Fig. 3). The segment 7 dsRNAs of the rSA11/NSP3-fNTD, -fRBD, -fExRBD,
151 and -fCR isolates contained foreign sequence insertions of 1.0, 0.7, 1.0, and 1.2 kbp,
152 respectively, significantly smaller than the 2.1 kbp foreign sequence insertion of rSA11/NSP3-
153 fS1. The smaller sizes of the foreign-sequence insert in the segment 7 RNAs of rSA11/NSP3-
154 fNTD, -fRBD, -fExRBD, and -fCR provide additional genetic space that can be used to add
155 routing and localization signals to S protein products, which may enhance their antigen
156 processing and presentation, recognition by T cells, and trafficking to immune cells. For
157 example, the extra genetic space can be used to add an N-terminal ER trafficking signal and a C-
158 terminal plasma-membrane localization signal to the ExRBD, along with internal coiled-coil
159 cassettes, that may favor surface presentation of a multimerized form of the ExRBD capable of
160 inducing enhanced production of SARS-CoV-2 neutralizing antibodies.

161 Consistent with previous studies examining the phenotypes of rSA11 isolates expressing
162 FPs (16-17), the sizes of plaques formed by rSA11/NSP3-CoV2/S viruses were smaller than
163 plaques formed by rSA11/wt. Similarly, rSA11 viruses containing S-protein coding sequences
164 grew to maximum titers that were up to 0.5-1 log lower than rSA11/wt. The reason for the

165 smaller plaques and lower titers of the rSA11/NSP3-CoV2/S viruses is unknown, but may reflect
166 the longer elongation time likely required for the viral RNA polymerase to transcribe their
167 segment 7 dsRNAs during viral replication. Alternatively, it may reflect the longer time required
168 to translate segment 7 (+)RNAs that contain S-protein coding sequences.

169 **Expression of S coding sequences by rSA11 rotaviruses.** To determine whether the
170 rSA11/NSP3-CoV2/S viruses expressed products from their S sequences, lysates prepared from
171 MA104 cells infected with these viruses were examined by immunoblot assay using FLAG- and
172 RBD-specific antibodies (Fig. 4A, B). Immunoblots probed with FLAG antibody showed that
173 rSA11/NSP3-fNTD, -fExRBD, -fRBD, and -fCR viruses generated S products and that their
174 sizes were as predicted for an active 2A element in the segment 7 ORF: fNTD (34.8 kDa),
175 fExRBD (35.2 kDa), fRBD (24.3 kDa), and fCR (42.9 kDa) (Table 1). Immunoblot assays
176 indicated that the rSA11/NSP3-fExRBD yielded higher levels of S product than any of the other
177 rSA11/NSP3-CoV2/S viruses. The basis for the higher levels of the fExRBD product is unclear,
178 but does not correlate with increased levels of expression of other viral products, such as NSP3
179 and VP6. Nonetheless, the high levels of ExRBD expression by rSA11/NSP3-fExRBD suggests
180 that such viruses may be best suited in pursuing the development of combined rotavirus/COVID
181 vaccines.

182 FLAG antibody did not detect the expected 79.6-kDa fS1 product in cells infected with
183 rSA11/NSP3-fS1 (Fig. 4A). The S1 coding sequence in the segment 7 ORF includes an N-
184 terminal signal sequence which, in SARS-CoV-2 infected cells, is cleaved from the S1 protein
185 during synthesis on the endoplasmic reticulum (ER) (29,38). Cleavage of the signal sequence
186 may have removed the upstream 3x FLAG tag from a S1 product, preventing its detection by the
187 FLAG antibody. It is also possible that glycosylation and/or degradation of the 79.6 kDa-S1

188 product by ER-associated proteases may have prevented the protein's detection. In addition,
189 rotavirus which usurps and possibly remodels the ER in support of glycoprotein (NSP4 and VP7)
190 synthesis and virus morphogenesis may perturb ER-interaction with the S signal sequence in
191 such a way to prevent S1 synthesis (21). Interestingly, all the rSA11/NSP3-CoV2/S viruses,
192 including rSA11/NSP3-fS1, generated 2A read-through products that were detectable using
193 FLAG antibody. Thus, the 2A stop-start element in the rSA11/NSP3-2A-CoV2/S viruses was not
194 fully active, which is consistent with previous reports analyzing the functionality of 2A elements
195 within cells (39-41). However, with the exception of the rSA11/NSP3-fS1, all the viruses
196 generated more 2A-cleaved S product than read-through product. Mutation of residues in and
197 around the 2A element, including the inclusion of flexible linker sequences, may decrease the
198 relative frequency of read through (42-43).

199 Lysates from MA104 cells infected with rSA11/wt, rSA11/NSP3-fRBD, and
200 rSA11/NSP3-fExRBD were also probed with a RBD-specific polyclonal antibody prepared
201 against a peptide mapping to the C-terminal end of the RBD domain (ProSci 9087). The RBD
202 antibody recognized the fExRBD product of the rSA11/NSP3-fExRBD virus, but not the fRBD
203 product of rSA11/NSP3-fRBD (Fig. 4B), presumably because the latter product lacked the
204 peptide sequence used in generating the ProSci RBD antibody. To gain insight into whether the
205 fRBD and fExRBD products folded into native structures mimicking those present in the SARS-
206 CoV-2 S protein, lysates prepared from MA104 cells infected with rSA11/NSP3-fRBD and
207 rSA11/NSP3-fExRBD were probed by pulldown assay using an anti-RBD conformation-
208 dependent neutralizing monoclonal antibody (GeneTex CR3022). As shown in Fig. 4C, the
209 CR3022 immunoprecipitate included fExRBD, indicating that this product included a
210 neutralizing epitope found in authentic SARS-CoV-2 S protein. Thus, at least some of the RBD

211 product of rSA11/NSP3-fExRBD has likely folded in a conformation capable of inducing a
212 protective antibody response. Unlike the successful pulldown of ExRBD with CR3022 antibody,
213 it was not clear if the antibody likewise immunoprecipitated the fRBD product of rSA11/NSP3-
214 fRBD. This uncertainty stems from the light chain of the CR3022 antibody obscuring the
215 electrophoretically closely-migrating fRBD product in immunoblot assays (Fig. 4C).

216 **Expression of the ExRBD and RBD products by rSA11s during rotavirus infection.**

217 To gain insight into fExRBD and fRBD expression during virus replication, MA104 cells were
218 infected with rSA11/wt, rSA11/NSP3-fExRBD or rSA11/NSP3-fRBD and then harvested at
219 intervals between 0 and 12 hr p.i. Analysis of the infected cell lysates by immunoblot assay
220 showed that fExRBD and fRBD were readily detectable by 4 h p.i., paralleling the expression of
221 rotavirus proteins NSP3 and VP6 (Fig. 5). Increased levels of fExRBD and fRBD were present at
222 8 and 12 h p.i., without obvious accumulation of FLAG-tagged products of smaller sizes. Thus,
223 the fExRBD and fRBD products appear to be relatively stable.

224 **Density of rSA11 virus particles containing S sequences.** The introduction of S
225 sequences into the rSA11/NSP3-CoV2/S viruses increased the size of their viral genomes by 1.0
226 to 2.5 kbp beyond that of SA11/wt. Assuming the rSA11/NSP3-CoV2/S viruses are packaged
227 efficiently and contain a complete constellation of 11 genome segments, the increased content of
228 dsRNA within the core of rSA11/NSP3-CoV2/S particles should cause their densities to be
229 greater than that of SA11/wt particles. To explore this possibility, rSA11/wt (18.6-kbp genome),
230 rSA11/NSP3-fExRBD (19.5 kbp) and rSA11/NSP3-fS1 (20.8 kbp) were amplified in MA104
231 cells. The infected-cell lysates were then treated with EDTA to convert rotavirus virions (triple-
232 layered particles) into double-layered particles (DLPs). The particles were centrifuged to
233 equilibrium on CsCl gradients (Fig. 6) and the density of the DLP bands determined by

234 refractometry. The analysis indicated that the density of rSA11/NSP3-fExRBD DLPs (1.386
235 g/cm³) was greater than SA11/wt DLPs (1.381 g/cm³) (panel A) and similarly, the density of
236 rSA11/NSP3-fS1 DLPs (1.387 g/cm³) was greater than SA11/wt DLPs (1.38 g/cm³) (panel B).
237 Analysis of the banded DLPs by gel electrophoresis confirmed that they contained the expected
238 constellation of eleven genome segments. To confirm that the density of rSA11/NSP3-fS1 DLPs
239 was different than rSA11/wt DLPs, infected-cell lysates containing each of these viruses were
240 pooled, treated with EDTA, and the viral DLPs in the combined sample banded by centrifugation
241 on a CsCl gradient (Fig. 6, panel E). Analysis of the gradient revealed the presence of two bands
242 of particles, indicating that rSA11/NSP3-fSA11-fS1 and rSA11/wt DLPs were of different
243 densities. Gel electrophoresis of the combined DLP bands showed, as expected, that both
244 rSA11/NSP3-fSA11-fS1 and rSA11/wt were present. Taken together, these results demonstrate
245 that rSA11/NSP3-CoV-2/S virions contain complete genome constellations despite the fact that
246 their genome sizes are significantly greater than that of wildtype SA11 virus. Indeed, the 20.8-
247 kbp rSA11/NSP3-fS1 genome is 12% greater in size than the 18.6-kbp rSA11/wt genome (Table
248 1). Thus, the rotavirus core has space to accommodate large amounts of additional foreign
249 sequence. How the dsRNA within the core is re-distributed to accommodate large amounts of
250 additional sequence is not known, but clearly the core remains a transcriptionally-active
251 nanomachine despite the additional sequence. Whether other genome segments can be
252 engineered similarly to segment 7 of rSA11/NSP3-fS1 to include 2 kb of additional sequence
253 remains to be determined. The maximum packaging capacity of the core also remains to be
254 determined.

255 **Genetic stability of rSA11 rotaviruses containing S sequences.** The genetic stability of
256 the rSA11/NSP3-CoV2/S viruses were assessed by serial passage, with a fresh monolayer of

257 MA104 cells infected with 1:1000 dilutions of cell lysates at each round. Electrophoretic analysis
258 of the dsRNAs recovered from cells infected with rSA11/NSP3-fNTD, -fRBD, -ExRBD, or -
259 ExCR showed no changes in the sizes of any of the 11 genome segments over 5 rounds of
260 passage (P1-P5), including segment 7, indicating that these viruses were genetically stable. In
261 contrast, serial passage of rSA11/NSP3-S1 showed evidence of instability. By the third round of
262 passage, novel genome segments were appearing that were smaller than the 3.3-kbp segment 7
263 RNA. With continued passage, four novel segments (R-1 to R-4) became prominent and the 3.3-
264 kbp segment 7 RNA was no longer detectable, suggesting that the high-passage virus pools (P3-
265 P6) were populated by variants containing segment 7 RNAs derived from the 3.3-kb segment 7
266 RNA through internal sequence deletion. To evaluate this possibility, 8 variants were recovered
267 from the P6 virus pool by plaque isolation, 4 with a large (L) plaque phenotype and 4 with a
268 small (S) plaque phenotype. Electrophoretic analysis of the genomes of the variants showed that
269 none contained the 3.3-kbp segment 7 RNA. Instead, 6 variants (L1, L2, L3, L4, S2, and S4)
270 contained the R3 segment, and the other two variants contained either the R1 (S1) or R2 (R2)
271 segment. No variants were recovered that contained the novel R4 segment. Sequencing showed
272 that the R1, R2, and R3 segments were in fact derivatives of the 3.3-kbp segment 7 RNA. The
273 R1, R2, and R3 RNAs all retained the complete 5'- and 3'-UTRs and NSP3 ORF of segment 7,
274 but contained sequence deletions of 1.0 (R1), 1.5 (R2), or 1.8 (R3) kbp of S1 coding sequence.
275 The fact that 6 of the 8 variants isolated by plaque assay contained the R3 segment suggests that
276 variants with this RNA may have a growth advantage over variants with the R1, R2, or R4
277 RNAs. Although genetic instability gave rise to rSA11/NSP3-fS1 variants lacking portions of the
278 S1 ORF, none were identified that lacked portions of the NSP3 ORF. This suggests that NSP3
279 may be essential for virus replication, which would explain the failure of previous efforts by us

280 to recover viable rSA11s encoding truncated forms of NSP3 through insertion of stop codons in
281 the NSP3 ORF (data not shown).

282 **Summary.** We have shown that reverse genetics can be used to generate recombinant
283 rotaviruses that express, as separate products, portions of the SARS-CoV-2 S protein, including
284 its immunodominant RBD. These results indicate that it may be possible to develop rotaviruses
285 as vaccine expression vectors, providing a path for generating oral live-attenuated rotavirus-
286 COVID-19 combination vaccines able to induce immunological protective responses against
287 both rotavirus and SARS-CoV-2. Such combination vaccines would be designed for use in
288 infants and young children and would allow the widespread distribution and administration of
289 COVID-19-targeted vaccines by piggy backing onto current rotavirus immunization programs
290 used in the USA and many other countries, both developed and developing. In addition, our
291 findings raise the possibility that through the use of rotavirus as vaccine expression platforms,
292 rotavirus-based combination vaccines could be made against other enteric viruses including
293 norovirus, astrovirus, and hepatitis E virus.

294 We have determined that the 18.6-kbp rotavirus dsRNA can accommodate as much as
295 2.2-kbp of foreign sequence, which is sufficient to encode the SARS-CoV-2 S1 protein.
296 However, in our hands, rSA11s encoding S1 were not genetically stable and failed to express the
297 appropriate S1 product, for reasons that are uncertain but under further investigation. Rotaviruses
298 carrying large amounts of foreign sequence are characteristically genetically unstable (this study
299 and data not shown), but those with foreign sequences of <1.0-1.5-kbp are stable over 5-10
300 rounds of serial passage at low MOI and, thus, can be developed into vaccine candidates . The
301 coding capacity provided by 1.0-1.5-kbp of extra sequence is sufficient to produce recombinant
302 rotaviruses that encode the SARS-CoV-2 NTD, RBD, or S2 core along with trafficking signals

303 that can promote engagement of S products with antigen-presenting cells and naive B-
304 lymphocytes. Current work is underway to gain insight how successful rotaviruses expressing
305 SARS-CoV-2 products are in inducing neutralizing antibodies in immunized animals.

306

307 **MATERIALS AND METHODS**

308 **Cell culture.** Embryonic monkey kidney cells (MA104) were grown in medium 199
309 (M199) containing 5% fetal bovine serum (FBS) and 1% penicillin-streptomycin. Baby hamster
310 kidney cells expressing T7 RNA polymerase (BHK-T7) were provided by Dr. Ulla Buchholz,
311 Laboratory of Infectious Diseases, NIAID, NIH, and were propagated in Glasgow minimum
312 essential media (GMEM) containing 5% heat-inactivated fetal bovine serum (FBS), 10%
313 tryptone-peptide broth, 1% penicillin-streptomycin, 2% non-essential amino acids, and 1%
314 glutamine (36). BHK-T7 cells were grown in medium supplemented with 2% Geneticin
315 (Invitrogen) with every other passage.

316 **Plasmid construction.** Recombinant SA11 rotaviruses were prepared using the plasmids
317 pT7/VP1SA11, pT7/VP2SA11, pT7/VP3SA11, pT7/VP4SA11, pT7/VP6SA11, pT7/VP7SA11,
318 pT7/NSP1SA11, pT7/NSP2SA11, pT7/NSP3SA11, pT7/NSP4SA11, and pT7/NSP5SA11
319 [https://www.addgene.org/Takeshi_Kobayashi/] and pCMV-NP868R (16). The plasmid
320 pT7/NSP3-P2A-fUnaG was produced, as described elsewhere, by fusing a DNA fragment
321 containing the ORF for P2A-3xFL-UnaG to the 3'-end of the NSP3 ORF in pT7/NSP3SA11
322 (17). A plasmid (pTWIST/COVID19spike) containing a full-length cDNA of the SARS-CoV-2 S
323 gene (GenBank MN908947.3) was purchased from Twist Bioscience. The plasmids pT7/NSP3-
324 2A-fNTD, pT7/NSP3-2A-fExRBD, pT7/NSP3-2A-fRBD, pT7/NSP3-2A-fCR, and pT7/NSP3-
325 2A-S1 were made by replacing the UnaG ORF in pT7/NSP3-2A-fUnaG with ORFs for the NTD,

326 ExRBD, RBD, CR, and S1 regions, respectively, of the SARS-CoV-2 S protein, by In-Fusion
327 cloning. DNA fragments containing NTD, ExRBD, RBD, CR, and S1 coding sequences were
328 amplified from pTWIST/COVID19spike using the primer pairs NTD_For and NTD_Rev,
329 ExRBD_For and ExRBD_Rev, RBD_For and RBD_Rev, CR_For and CR_Rev, and S1_For and
330 S1_Rev, respectively (Table 2). Transfection quality plasmids were prepared commercially
331 (www.plasmid.com) or using Qiagen plasmid purification kits. Primers were provided by and
332 sequences determined by EuroFins Scientific.

333 **Recombinant viruses.** The reverse genetics protocol used to generate recombinant
334 rotaviruses was described in detail previously (16,44). To summarize, BHK-T7 cells were
335 transfected with SA11 pT7 plasmids and pCMV-NP868R using Mirus TransIT-LT1 transfection
336 reagent. Two days later, the transfected cells were overseeded with MA104 cells and the growth
337 medium (serum-free) adjusted to a final concentration of 0.5 µg/ml trypsin. Three days later, the
338 BHK-T7/MA104 cell mixture was freeze-thawed 3-times and the lysates clarified by low-speed
339 centrifugation. Recombinant virus in clarified lysates were amplified by one or two rounds of
340 passage in MA104 cells maintained in serum-free medium containing 0.5 µg/ml trypsin.
341 Individual virus isolates were obtained by plaque purification and typically amplified 1 or 2
342 rounds in MA104 cells prior to analysis. Viral dsRNAs were recovered from infected-cell lysates
343 by Trizol extraction, resolved by electrophoresis on Novex 8% polyacrylamide gels (Invitrogen)
344 in Tris-glycine buffer, and detected by staining with ethidium bromide. Viral dsRNAs in gels
345 were visualized using a BioRad ChemiDoc MP Imaging System. The genetic stability of plaque
346 isolated rSA11s was assessed by serial passage as described previously (17).

347 **Immunoblot analysis.** MA104 cells were mock infected or infected with 5 PFU of
348 recombinant virus per cell and harvested at 8 h p.i. Cells were washed with cold phosphate-

349 buffered saline (PBS), pelleted by low-speed centrifugation, and lysed by resuspending in lysis
350 buffer [300 mM NaCl, 100 mM Tris-HCl, pH 7.4, 2% Triton X-100, and 1x EDTA-free protease
351 inhibitor cocktail (Roche cOmplete)]. For immunoblot assays, lysates were resolved by
352 electrophoresis on Novex linear 8-16% polyacrylamide gels and transferred to nitrocellulose
353 membranes. After blocking with phosphate-buffered saline containing 5% non-fat dry milk, blots
354 were probed with guinea pig polyclonal NSP3 (Lot 55068, 1:2000) or VP6 (Lot 53963, 1:2000)
355 antisera (2), mouse monoclonal FLAG M2 (Sigma F1804, 1:2000), rabbit monoclonal PCNA
356 [13110S, Cell Signaling Technology (CST), 1:1000] antibody or rabbit anti-RBD (ProSci 9087;
357 1:200) antibody. Primary antibodies were detected using 1:10,000 dilutions of horseradish
358 peroxidase (HRP)-conjugated secondary antibodies: horse anti-mouse IgG (CST), anti-guinea
359 pig IgG (KPL), or goat anti-rabbit IgG (CST). Signals were developed using Clarity Western
360 ECL Substrate (Bio-Rad) and detected using a Bio-Rad ChemiDoc imaging system.

361 **Immunoprecipitation assay.** Mock-infected and infected cell lysates were prepared as
362 above. Lysates were mixed with a SARS-CoV-2 S1 specific monoclonal antibody (GeneTex
363 CR3022, 1:150 dilution) or an NSP2 monoclonal antibody (#171, 1:200). After incubation at 4C
364 with gentle rocking for 18 h, antigen-antibody complexes were recovered using Pierce magnetic
365 IgA/IgG beads (ThermoFisher Scientific), resolved by gel electrophoresis, and blotted onto
366 nitrocellulose membranes. Blots were probed with FLAG antibody (1:2000) to detect fRBD and
367 fExRBD and NSP2 antibody (1:2000).

368 **CsCl gradient centrifugation.** MA104-cell monolayers in 10-cm cell culture plates were
369 infected with rSA11 viruses at an MOI of 5 and harvested at 12 h p.i. Cells were lysed by
370 adjusting media to 0.5% Triton X100 (Sigma) and incubation on ice for 5 min. Lysates were then
371 clarified by centrifugation at 500 x g at 4C for 6 min. The clarified lysates were adjusted to 10

372 mM EDTA and incubated for 1 h at 37C to cause the conversion of rotavirus TLPs to DLPs (36).
373 CsCl was added to samples to a density of 1.367 g/cm³ and samples were centrifuged at 110,000
374 x g with a Beckman SW55Ti rotor at 8C for 22 h. Fractions containing viral bands were
375 recovered using a micropipettor and fraction densities were determined using a refractometer.

376 **Genetic stability of rSA11 viruses.** Viruses were serially passaged on MA104-cell
377 monolayers using 1:1000 dilutions of infected cell lysates prepared in serum-free M199 medium
378 and 0.5 µg/ml trypsin. When cytopathic effects reached completion (4-5 days), cells were freeze-
379 thawed twice in their medium, and lysates were clarified by low-speed centrifugation. To recover
380 dsRNA, clarified lysates (600 ul) were extracted with Trizol (ThermoFisher Scientific). The
381 RNA samples were resolved by electrophoresis on 8% polyacrylamide gels and the bands of
382 dsRNA detected by ethidium-bromide staining.

383 **GenBank accession numbers.** Segment 7 sequences in rSA11 viruses have been
384 deposited in Genbank: wt (LC178572), NSP3-P2A-fNTD (MW059024), NSP3-P2A-fRBD
385 (MT655947), NSP3-P2A-ExRBD (MT655946), NSP3-P2A-fCR (MW059025), NSP3-P2A-S1
386 (MW059026), NSP3-P2A-S1/R1 (MW353715), NSP3-P2A-S1/R2 (MW353716), and NSP3-
387 P2A-S1/R3 (MW353717). See also Table 1.

388

389 **ACKNOWLEDGEMENT**

390 Our thanks go to lab members for their support and encouragement on this project. This
391 work was funded by National Institutes of Health grant R21AI144881, Indiana University Start-
392 Up Funding, and the Lawrence M. Blatt Endowment.

393 **FIGURE LEGENDS**

394 **Figure 1. Domains of the SARS-CoV-2 S protein expressed by rSA11.** (A) S protein trimers
395 are cleaved at the S1/S2 junction by furin proconvertase and at the S2' site by the TMPRSS2
396 serine protease. The S1 fragment contains a signal sequence (SS), N-terminal domain (NTD),
397 receptor binding domain (RBD), and receptor binding motif (RBM). The S2 fragment contains a
398 trimeric core region, transmembrane anchor (TM), and fusion domain. (B) Portions of the S
399 protein expressed by recombinant rotaviruses are indicated. (C) Ribbon representations of the
400 closed conformation of the trimeric S protein (PDB 6VXX) showing locations of the RBD
401 (magenta), extended RBD (ExRBD, cyan), NTD (blue), core (CR, gold) domains and the S1
402 cleavage product (green).

403 **Figure 2. Plasmids with modified segment 7 (NSP3) cDNAs used to generate rSA11 viruses**
404 **expressing regions of the SARS-CoV-2 S protein.** Illustration indicates nucleotide positions of
405 the coding sequences for NSP3, porcine teschovirus 2A element, 3xFLAG (FL), and the
406 complete S1 or portions of the S1 (NTD, ExRBD, and RBD) and S2 (CR) proteins. The red
407 arrow notes the position of the 2A translational stop-restart site, and the asterisk notes the end of
408 the ORF. Sizes (aa) of encoded NSP3 and S products are in parenthesis. T7 (T7 RNA
409 polymerase promoter sequence), Rz (Hepatitis D virus ribozyme), UTR (untranslated region).

410 **Figure 3. Properties of rSA11/NSP3-CoV2/S viruses expressing regions of the SARS-CoV-2**
411 **S protein.** (A and B) dsRNA was recovered from MA104 cells infected with plaque-purified
412 rSA11 isolates, resolved by gel electrophoresis, and detected by ethidium-bromide staining.
413 RNA segments of rSA11/wt are labeled 1 to 11. Sizes (kbp) of segment 7 RNAs (black arrows)
414 of rSA11 isolates are indicated. Double-stranded RNA of rSA11/NSP3-fS1 serially passaged
415 twice (P1 and P2) in MA104 cells is shown in (A). (C) Plaque assays were performed using

416 MA104 cells and detected by crystal-violet staining. **(D)** Titers reached by rSA11 isolates were
417 determined by plaque assay. Bars indicate standard deviations calculated from three separate
418 determinations.

419 **Figure 4. Expression of SARS-CoV-2 S products by rSA11 viruses.** **(A, B)** Whole cell lysates
420 (WCL) were prepared from cells infected with rSA11 viruses and examined by immunoblot
421 assay using **(A)** FLAG antibody to detect S products (NTD, ExRBD, RBD, CR, S1, and 2A read-
422 through products) and antibodies specific for rotavirus NSP3 and VP6 and cellular PCNA. Red
423 asterisks identify 2A read-through products and blue asterisks identify 2A cleavage products. **(B)**
424 Lysates prepared from MA104 cells infected with rSA11wt, rSA11/NSP3-fRBD and
425 rSA11/NSP3-fExRBD were examined by immunoblot assay using antibodies specific for RBD
426 (ProSci 9087), rotavirus VP6, and PCNA. **(C)** Lysates prepared from MA104 cells infected with
427 rSA11/wt, rSA11/NSP3-fRBD and rSA11/NSP3-fExRBD viruses were examined by
428 immunoprecipitation assay using a SARS-CoV-2 S1 specific monoclonal antibody (GeneTex
429 CR3022). Lysates were also analyzed with a NSP2-specific polyclonal antibody. Antigen-
430 antibody complexes were recovered using IgA/G beads, resolved by gel electrophoresis, blotted
431 onto nitrocellulose membranes, and probed with FLAG (fRBD and fExRBD) and NSP2
432 antibody. Molecular weight markers are indicated (kDa). Red arrows indicate fRBD and
433 fExRBD. fRBD comigrates near the Ig light chain (Ig/L). Ig heavy chain, Ig/H).

434 **Figure 5. Production of RBD and ExRBD by rSA11 viruses during infection.** MA104 cells
435 were mock infected or infected with rSA11/wt, rSA11/NSP3-fRBD, or rSA11/NSP3-fExRBD
436 (MOI of 5). Lysates were prepared from the cells at 0, 4, 8, or 12 h p.i. and analyzed by
437 immunoblot assay using antibodies specific for FLAG, NSP3, VP6, and PCNA. Red asterisks
438 identify 2A read-through products. Positions of molecular weight markers are indicated (kDa).

439 **Figure 6. Impact of genome size on rotavirus particle density.** MA104 cells were infected
440 with rSA11/wt, rSA11/NSP3-fExRBD, or rSA11/NSP3-fS1 viruses at an MOI of 5. At 12 h p.i.,
441 the cells were recovered, lysed by treatment with non-ionic detergent, and treated with EDTA to
442 convert rotavirus virions into DLPs. **(A, B)** DLPs were banded by centrifugation in CsCl
443 gradients and densities (g/cm^3) were determined using a refractometer. **(C)** Lysates from
444 rSA11/wt and rSA11/NSP3-fS1 infected cells were combined and their DLP components banded
445 by centrifugation in a CsCl gradient. **(D, E)** Electrophoretic profile of the dsRNA genomes of
446 DLPs recovered from CsCl gradients. Panel D RNAs derive from DLPs in panel A and panel E
447 RNAs derive from DLPs in panel B and C. RNA segments of rSA11/wt are labeled 1 to 11.
448 Positions of segment 7 RNAs are indicated with red arrows.

449 **Figure 7. Genetic stability of rSA11 strains expressing SARS-CoV-2 S domains.** rSA11
450 strains were serially passaged 5 to 6 times (P1 to P5 or P6) in MA104 cells. **(A)** Genomic RNAs
451 were recovered from infected cell lysates and analyzed by gel electrophoresis. Positions of viral
452 genome segments are labeled. Position of modified segment 7 (NSP3) dsRNAs introduced into
453 rSA11 strains are denoted with black arrows. Genetic instability of the modified segment 7
454 (NSP3) dsRNA of rSA11/NSP3-fS1 yielded R1-R4 RNAs during serial passage. **(B)** Genomic
455 RNAs prepared from large (L1-L4) and small (S1-S4) plaque isolates of P6 rSA11/NSP3-fS1.
456 Segment 7 RNAs are identified as R1-R3, as in **(A)**. **(C)** Organization of R1-R3 sequences
457 determined by sequencing of segment 7 RNAs of L1, S1, and S3 plaque isolates. Sequence
458 deletions are indicated with dashed lines. Regions of the S1 ORF that are no longer encoded by
459 the R1-R3 segment 7 RNAs are indicated by slashed green-white boxes.

460

461 **References**

- 462 1. Dai L, Gao GF. 2021. Viral targets for vaccines against COVID-19. *Nat Rev Immunol* 21,
463 73–82.
- 464 2. Kaur SP, Gupta V. 2020. COVID-19 Vaccine: A comprehensive status report. *Virus*
465 *Research* 288: 198114.
- 466 3. Ludvigsson JF. 2020. Systematic review of COVID-19 in children shows milder cases and a
467 better prognosis than adults. *Acta Paediatr* 109(6):1088-1095.
- 468 4. Pollán M, Pérez-Gómez B, Pastor-Barriuso R, Oteo J, Hernán MA, Pérez-Olmeda M,
469 Sanmartín JL, Fernández-García A, Cruz I, Fernández de Larrea N, Molina M, Rodríguez-
470 Cabrera F, Martín M, Merino-Amador P, León Paniagua J, Muñoz-Montalvo JF, Blanco F,
471 Yotti R; ENE-COVID Study Group. 2020. Prevalence of SARS-CoV-2 in Spain (ENE-
472 COVID): a nationwide, population-based seroepidemiological study. *Lancet* 396 (10250):
473 535-544.
- 474 5. Burke RM, Tate JE, Kirkwood CD, Steele AD, Parashar UD. 2019. Current and new
475 rotavirus vaccines. *Curr Opin Infect Dis* 32: 435-444.
- 476 6. Folorunso OS, Sebolai OM. 2020. Overview of the development, impacts, and challenges of
477 live-attenuated oral rotavirus vaccines. *Vaccines (Basel)* 8(3): 341.
- 478 7. Ali A, Kazi AM, Cortese MM, Fleming JA, Moon S, Parashar UD, Jiang B, McNeal MM,
479 Steele D, Bhutta Z, Zaidi AK. 2015. Impact of withholding breastfeeding at the time of
480 vaccination on the immunogenicity of oral rotavirus vaccine--a randomized trial. *PLoS One*
481 10(6): e0127622. Erratum in: *PLoS One* 10(12): e0145568.

- 482 8. Liu GF, Hille D, Kaplan SS, Goveia MG. 2017. Postdose 3 G1 serum neutralizing antibody
483 as correlate of protection for pentavalent rotavirus vaccine. *Hum Vaccin Immunother* 13(10):
484 2357-2363.
- 485 9. Angel J, Steele AD, Franco MA. 2014. Correlates of protection for rotavirus vaccines:
486 Possible alternative trial endpoints, opportunities, and challenges. *Hum Vaccin Immunother*
487 10(12): 3659-71.
- 488 10. Leshem E, Tate JE, Steiner CA, Curns AT, Lopman BA, Parashar UD. 2015. Acute
489 gastroenteritis hospitalizations among US children following implementation of the rotavirus
490 vaccine. *JAMA*. 2015 313(22): 2282-4. Erratum in: *JAMA* 314(2): 188.
- 491 11. Clark A, Black R, Tate J, Roose A, Kotloff K, Lam D, Blackwelder W, Parashar U, Lanata
492 C, Kang G, Troeger C, Platts-Mills J, Mokdad A; Global Rotavirus Surveillance Network,
493 Sanderson C, Lamberti L, Levine M, Santosham M, Steele D. 2017. Estimating global,
494 regional and national rotavirus deaths in children aged <5 years: Current approaches, new
495 analyses and proposed improvements. *PLoS One* 12(9): e0183392.
- 496 12. Kanai Y, Kawagishi T, Nouda R, Onishi M, Pannacha P, Nurdin JA, Nomura K, Matsuura,
497 Y, Kobayashi T. 2018. Development of stable rotavirus reporter expression systems. *J Virol*
498 93: e01774-18.
- 499 13. Komoto S, Fukuda S, Ide T, Ito N, Sugiyama M, Yoshikawa T, Murata T, Taniguchi K.
500 2018. Generation of recombinant rotaviruses expressing fluorescent proteins by using an
501 optimized reverse genetics system. *J Virol* 92: e00588-18.
- 502 14. Sánchez-Tacuba L, Feng N, Meade NJ, Mellits KH, Jaïs PH, Yasukawa LL, Resch TK, Jiang
503 B, López S, Ding S, Greenberg HB. 2020. An optimized reverse genetics system suitable for
504 efficient recovery of simian, human, and murine-like rotaviruses. *J Virol* 94(18): e01294-20.

- 505 15. Philip AA, Herrin BE, Garcia ML, Abad AT, Katen SP, Patton JT. 2019. Collection of
506 recombinant rotaviruses expressing fluorescent reporter proteins. *Microbio Resour Announc*
507 8(27): e00523-19.
- 508 16. Philip AA, Perry JL, Eaton HE, Shmulevitz M, Hyser JM, Patton JT. 2019. Generation of
509 recombinant rotavirus expressing NSP3-UnaG fusion protein by a simplified reverse genetics
510 system. *J Virol* 93: e01616-19.
- 511 17. Philip AA, Patton JT. 2020. Expression of separate heterologous proteins from the rotavirus
512 NSP3 genome segment using a translational 2A stop-restart element. *J Virol* 94(18): e00959-
513 20.
- 514 18. Kanai Y, Komoto S, Kawagishi T, Nouda R, Nagasawa N, Onishi M, Matsuura Y, Taniguchi
515 K, Kobayashi T. 2017. Entirely plasmid-based reverse genetics system for rotaviruses. *Proc*
516 *Natl Acad Sci USA* 114: 2349-2354.
- 517 19. Komoto S, Fukuda S, Kugita M, Hatazawa R, Koyama C, Katayama K, Murata T, Taniguchi
518 K. 2019. Generation of infectious recombinant human rotaviruses from just 11 cloned
519 cDNAs encoding the rotavirus genome. *J Virol* 93(8): e02207-18.
- 520 20. Crawford SE, Ramani S, Tate JE, Parashar UD, Svensson L, Hagbom M, Franco MA,
521 Greenberg HB, O'Ryan M, Kang G, Desselberger U, Estes MK. 2017. Rotavirus infection.
522 *Nat Rev Dis Primers* 3: 17083.
- 523 21. Trask SD, McDonald SM, Patton JT. 2012. Structural insights into the coupling of virion
524 assembly and rotavirus replication. *Nat Rev Microbiol* 10: 165–177.
- 525 22. Eaton HE, Kobayashi T, Dermody TS, Johnston RN, Jais PH, Shmulevitz M 2017. African
526 swine fever virus NP868R capping enzyme promotes reovirus rescue during reverse genetics

- 527 by promoting reovirus protein expression, virion assembly, and RNA incorporation into
528 infectious virions. *J Virol* 91: e02416-16.
- 529 23. Criglar JM, Crawford SE, Zhao B, Smith HG, Stossi F, Estes MK. 2020. A genetically
530 engineered rotavirus NSP2 phosphorylation mutant impaired in viroplasm formation and
531 replication shows an early interaction between vNSP2 and cellular lipid droplets. *J Virol*
532 94(15): e00972-20.
- 533 24. Navarro, A., Trask, S.D., Patton, J.T. 2013. Generation of genetically stable recombinant
534 rotaviruses containing novel genome rearrangements and heterologous sequences by reverse
535 genetics. *J Virol* 87: 6211-6220.
- 536 25. Chang-Graham AL, Perry JL, Strtak AC, Ramachandran NK, Criglar JM, Philip AA, Patton
537 JT, Estes MK, Hyser JM. 2019. Rotavirus calcium dysregulation manifests as dynamic
538 calcium signaling in the cytoplasm and endoplasmic reticulum. *Sci Rep* 9(1):10822.
- 539 26. Komoto S, Kanai Y, Fukuda S, Kugita M, Kawagishi T, Ito N, Sugiyama M, Matsuura Y,
540 Kobayashi T, Taniguchi K. 2017. Reverse genetics system demonstrates that rotavirus
541 nonstructural protein NSP6 is not essential for viral replication in cell culture. *J Virol* 91:
542 e00695-17.
- 543 27. Gratia M, Sarot E, Vende P, Charpilienne A, Baron CH, Duarte M, Pyronnet S, Poncet D.
544 2015. Rotavirus NSP3 is a translational surrogate of the poly(A)-binding protein-poly(A)
545 complex. *J Virol* 89: 8773-8782.
- 546 28. Piron M, Delaunay T, Grosclaude J, Poncet D. 1999. Identification of the RNA-binding,
547 dimerization, and eIF4GI-binding domains of rotavirus nonstructural protein NSP3. *J Virol*
548 73: 5411-5421.

- 549 29. Duan L, Zheng Q, Zhang H, Niu Y, Lou Y, Wang H. 2020. The SARS-CoV-2 spike
550 glycoprotein biosynthesis, structure, function, and antigenicity: implications for the design of
551 spike-based vaccine immunogens. *Front Immunol* 11: 576622.
- 552 30. Huang Y, Yang C, Xu XF, Xu W, Liu SW. 2020. Structural and functional properties of
553 SARS-CoV-2 spike protein: potential antiviral drug development for COVID-19. *Acta*
554 *Pharmacol Sin* 41(9): 1141-1149.
- 555 31. Medina-Enríquez MM, Lopez-León S, Carlos-Escalante JA, Aponte-Torres Z, Cuapio A,
556 Wegman-Ostrosky T. 2020. ACE2: the molecular doorway to SARS-CoV-2. *Cell Biosci*
557 10(1): 148.
- 558 32. Rogers TF, Zhao F, Huang D, Beutler N, Burns A, He WT, Limbo O, Smith C, Song G,
559 Woehl J, Yang L, Abbott RK, Callaghan S, Garcia E, Hurtado J, Parren M, Peng L, Ramirez
560 S, Ricketts J, Ricciardi MJ, Rawlings SA, Wu NC, Yuan M, Smith DM, Nemazee D, Teijaro
561 JR, Voss JE, Wilson IA, Andrabi R, Briney B, Landais E, Sok D, Jardine JG, Burton DR.
562 2020. Isolation of potent SARS-CoV-2 neutralizing antibodies and protection from disease in
563 a small animal model. *Science* 369(6506): 956-963.
- 564 33. Graham C, Seow J, Huettner I, Khan H, Kouphou N, Acors S, Winstone H, Pickering S,
565 Pedro Galao R, Jose Lista M, Jimenez-Guardeno JM, Laing AG, Wu Y, Joseph M, Muir L,
566 Ng WM, Duyvesteyn HME, Zhao Y, Bowden TA, Shankar-Hari M, Rosa A, Cherepanov P,
567 McCoy LE, Hayday AC, Neil SJD, Malim MH, Doores KJ. 2021. Impact of the B.1.1.7
568 variant on neutralizing monoclonal antibodies recognizing diverse epitopes on SARS-CoV-2
569 Spike. *bioRxiv [Preprint]*. 2021 Feb 3:2021.02.03.429355.
- 570 34. Xiaojie S, Yu L, Lei Y, Guang Y, Min Q. 2021. Neutralizing antibodies targeting SARS-
571 CoV-2 spike protein. *Stem cell research* 50: 102125.

- 572 35. Liu L, Wang P, Nair MS, Yu J, Rapp M, Wang Q, Luo Y, Chan JF, Sahi V, Figueroa A, Guo
573 XV, Cerutti G, Bimela J, Gorman J, Zhou T, Chen Z, Yuen KY, Kwong PD, Sodroski JG,
574 Yin MT, Sheng Z, Huang Y, Shapiro L, Ho DD. 2020. Potent neutralizing antibodies against
575 multiple epitopes on SARS-CoV-2 spike. *Nature* 584(7821): 450-456.
- 576 36. Arnold M, Patton JT, McDonald SM. 2009. Culturing, storage, and quantification of
577 rotaviruses. *Curr Protoc Microbiol* Chapter 15: Unit 15C.3.
- 578 37. Desselberger U. 2020. What are the limits of the packaging capacity for genomic RNA in
579 the cores of rotaviruses and of other members of the Reoviridae? *Virus Res.* 276:197822.
- 580 38. Meyer B, Chiaravalli J, Gellenoncourt S, Brownridge P, Bryne DP, Daly LA, Walter M,
581 Agou F, Chakrabarti LA, Craik CS, Evers CE, Evers PA, Gambin Y, Sierecki E, Verdin E,
582 Vignuzzi M, Emmott E. 2020. Characterisation of protease activity during SARS-CoV-2
583 infection identifies novel viral cleavage sites and cellular targets for drug repurposing.
584 *bioRxiv* 2020.09.16.297945.
- 585 39. Roulston C, Luke GA, de Felipe P, Ruan L, Cope J, Nicholson J, Sukhodub A, Tilsner J,
586 Ryan MD. 2016. '2A-like' signal sequences mediating translational recoding: a novel form of
587 dual protein targeting. *Traffic* 17(8): 923-39.
- 588 40. Luke G, Escuin H, De Felipe P, Ryan M. 2010. 2A to the fore - research, technology and
589 applications. *Biotechnol Genet Eng Rev* 26: 223-60.
- 590 41. Liu Z, Chen O, Wall J, Zheng M, Zhou Y, Wang L, Vaseghi HR, Qian L, Liu J. 2017.
591 Systematic comparison of 2A peptides for cloning multi-genes in a polycistronic vector.
592 *Scientific reports* 7(1): 2193.

- 593 42. Sharma P, Yan F, Doronina VA, Escuin-Ordinas H, Ryan MD, Brown JD. 2012. 2A peptides
594 provide distinct solutions to driving stop-carry on translational recoding. *Nucleic Acids Res.*
595 40(7): 3143-51.
- 596 43. Shaimardanova AA, Kitaeva KV, Abdrakhmanova II, Chernov VM, Rutland CS, Rizvanov
597 AA, Chulpanova DS, Solovyeva VV. 2019. Production and application of multicistronic
598 constructs for various human disease therapies. *Pharmaceutics* 11(11): 580.
- 599 44. Philip AA, Dai J, Katen SP, Patton JT. 2020. Simplified reverse genetics method to recover
600 recombinant rotaviruses expressing reporter proteins. *J Vis Exp* 158: e61039.
- 601 45. Matthijssens J, Ciarlet M, McDonald SM, Attoui H, Bányai K, Brister JR, Buesa J, Esona,
602 MD, Estes MK, Gentsch JR, Iturriza-Gómara M, Johne R, Kirkwood CD, Martella V,
603 Mertens PP, Nakagomi O, Parreño V, Rahman M, Ruggeri FM, Saif LJ, Santos N, Steyer A.,
604 Taniguchi K, Patton JT, Desselberger U, Van Ranst M. 2011. Uniformity of rotavirus strain
605 nomenclature proposed by the Rotavirus Classification Working Group (RCWG). *Arch Virol*
606 156: 1397-1413.
- 607

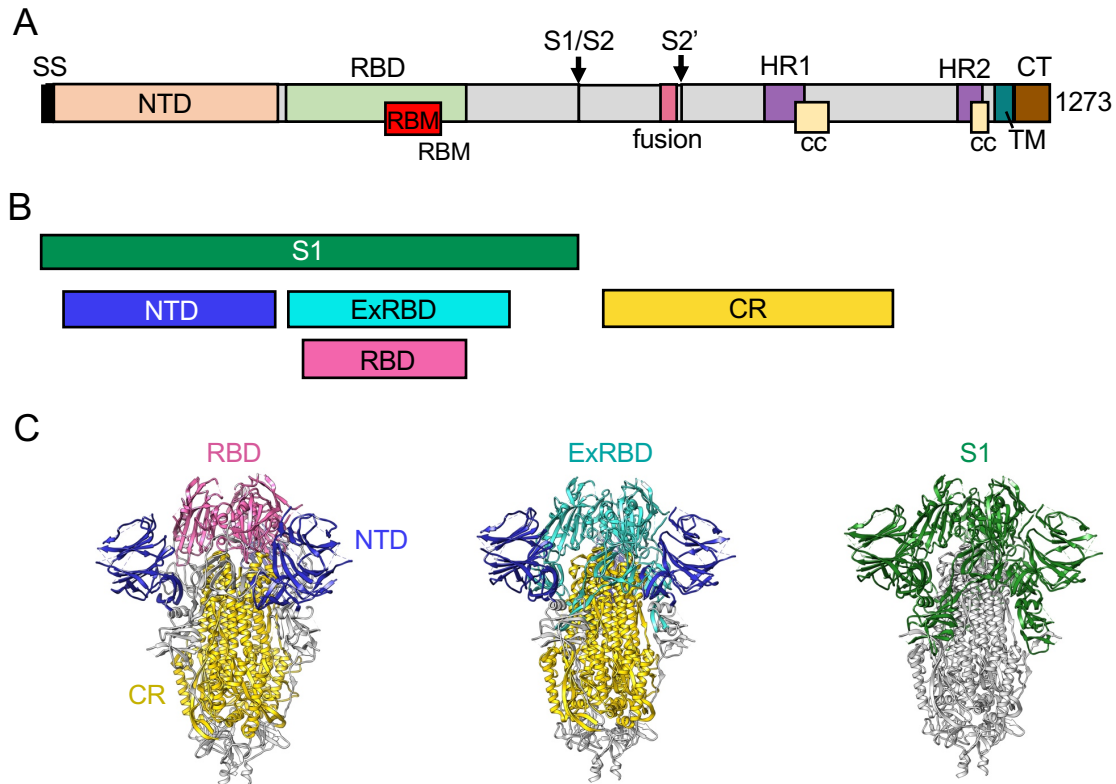


Figure 1. Domains of the SARS-CoV-2 S protein expressed by rSA11. (A) S protein trimers are cleaved at the S1/S2 junction by furin proconvertase and at the S2' site by the TMPRSS2 serine protease. The S1 fragment contains a signal sequence (SS), N-terminal domain (NTD), receptor binding domain (RBD), and receptor binding motif (RBM). The S2 fragment contains a trimeric core region, transmembrane anchor (TM), and fusion domain. (B) Portions of the S protein expressed by recombinant rotaviruses are indicated. (C) Ribbon representations of the closed conformation of the trimeric S protein (PDB 6VXX) showing locations of the RBD (magenta), extended RBD (ExRBD, cyan), NTD (blue), core (CR, gold) domains and the S1 cleavage product (green).

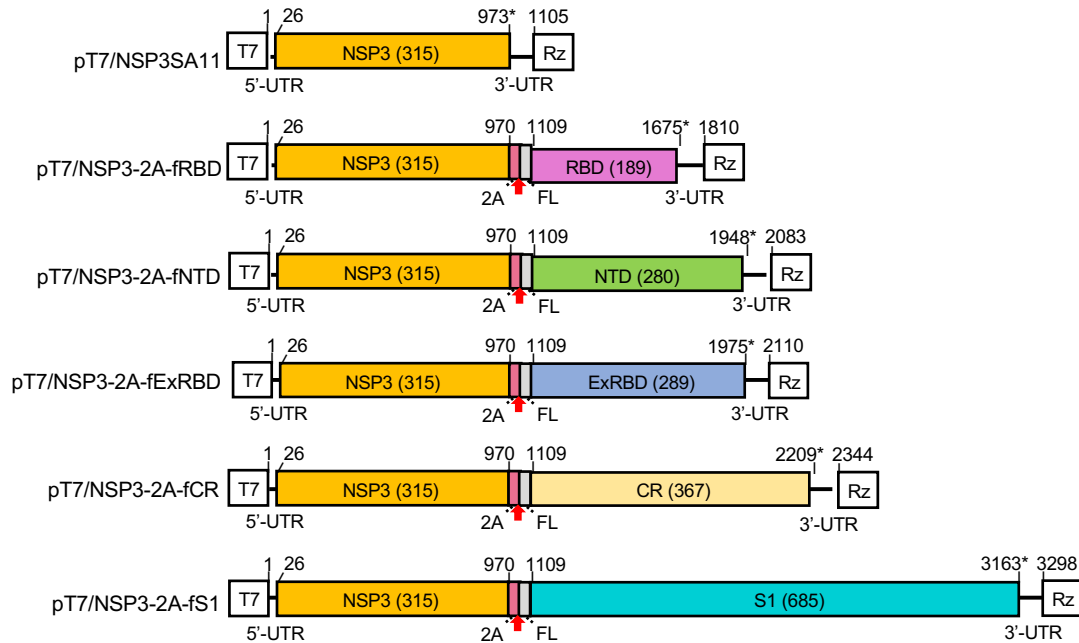


Figure 2. Plasmids with modified segment 7 (NSP3) cDNAs used to generate rSA11 viruses expressing regions of the SARS-CoV-2 S protein. Illustration indicates nucleotide positions of the coding sequences for NSP3, porcine teschovirus 2A element, 3xFLAG (FL), and the complete S1 or portions of the S1 (NTD, ExRBD, and RBD) and S2 (CR) proteins. The red arrow notes the position of the 2A translational stop-restart site, and the asterisk notes the end of the ORF. Sizes (aa) of encoded NSP3 and S products are in parenthesis. T7 (T7 RNA polymerase promoter sequence), Rz (Hepatitis D virus ribozyme), UTR (untranslated region).

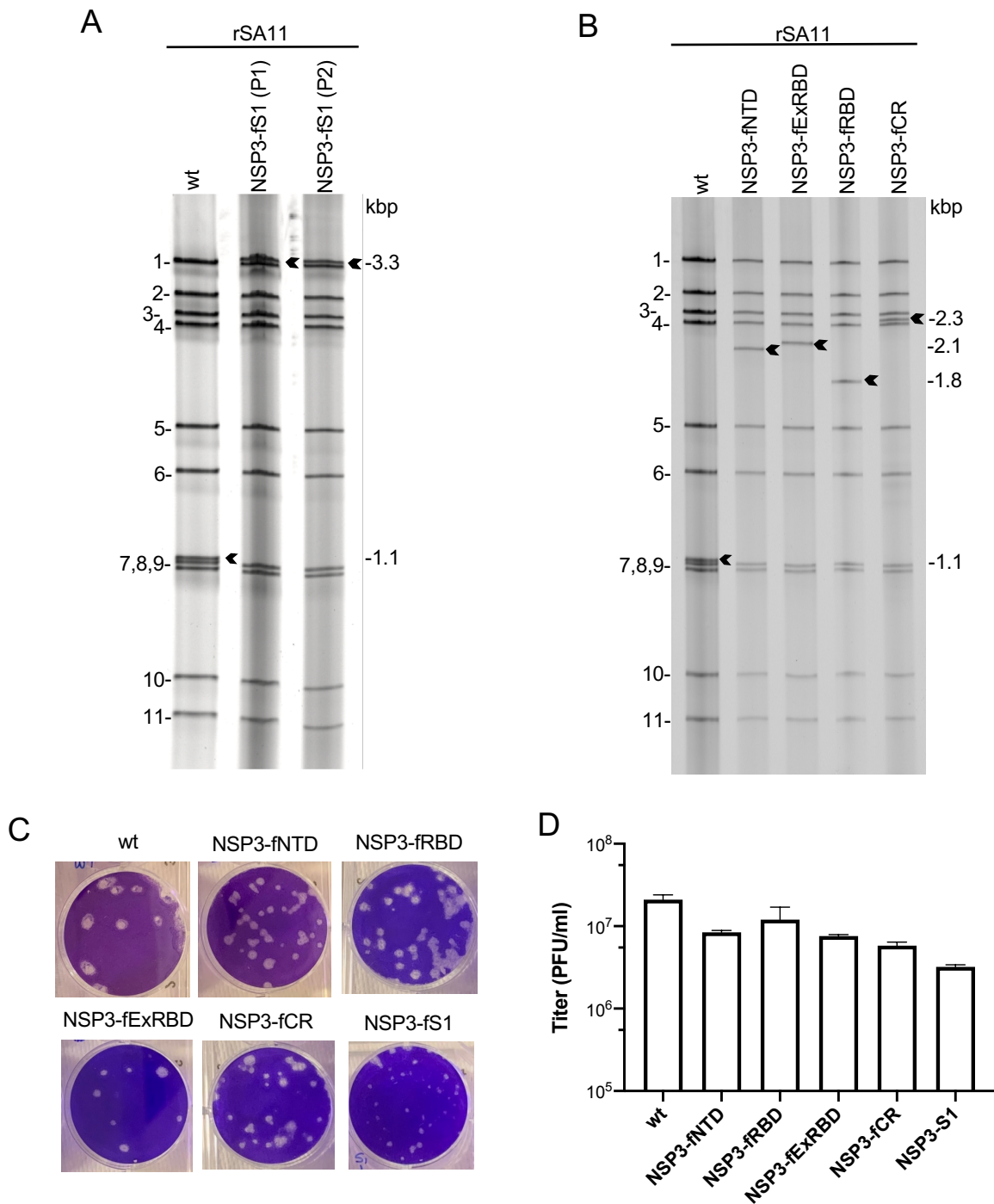


Figure 3. Properties of rSA11/NSP3-CoV2/S viruses expressing regions of the SARS-CoV-2 S protein. (A and B) dsRNA was recovered from MA104 cells infected with plaque-purified rSA11 isolates, resolved by gel electrophoresis, and detected by ethidium-bromide staining. RNA segments of rSA11/wt are labeled 1 to 11. Sizes (kbp) of segment 7 RNAs (black arrows) of rSA11 isolates are indicated. Double-stranded RNA of rSA11/NSP3-fS1 serially passaged twice (P1 and P2) in MA104 cells is shown in (A). (C) Plaque assays were performed using MA104 cells and detected by crystal-violet staining. (D) Titers reached by rSA11 isolates were determined by plaque assay. Bars indicate standard deviations calculated from three separate determinations.

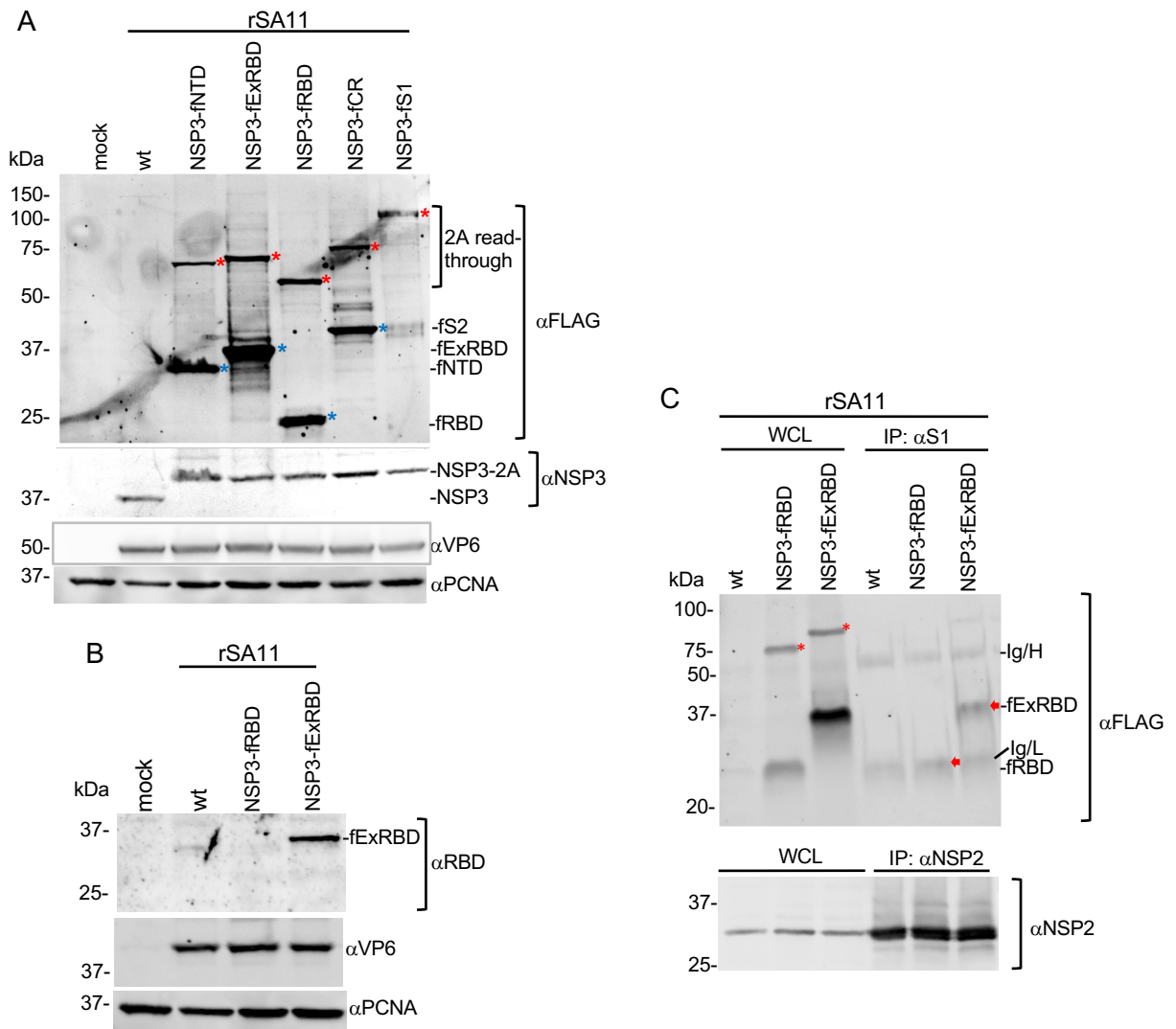


Figure 4. Expression of SARS-CoV-2 S products by rSA11 viruses. (A, B) Whole cell lysates (WCL) were prepared from cells infected with rSA11 viruses and examined by immunoblot assay using **(A)** FLAG antibody to detect S products (NTD, ExRBD, RBD, CR, S1, and 2A read-through products) and antibodies specific for rotavirus NSP3 and VP6 and cellular PCNA. Red asterisks identify 2A read-through products and blue asterisks identify 2A cleavage products. **(B)** Lysates prepared from MA104 cells infected with rSA11 wt, rSA11/NSP3-fRBD and rSA11/NSP3-fExRBD were examined by immunoblot assay using antibodies specific for RBD (ProSci 9087), rotavirus VP6, and PCNA. **(C)** Lysates prepared from MA104 cells infected with rSA11/wt, rSA11/NSP3-fRBD and rSA11/NSP3-fExRBD viruses were examined by immunoprecipitation assay using a SARS-CoV-2 S1 specific monoclonal antibody (GeneTex CR3022). Lysates were also analyzed with a NSP2-specific polyclonal antibody. Antigen-antibody complexes were recovered using IgA/G beads, resolved by gel electrophoresis, blotted onto nitrocellulose membranes, and probed with FLAG (fRBD and fExRBD) and NSP2 antibody. Molecular weight markers are indicated (kDa). Red arrows indicate fRBD and fExRBD. fRBD comigrates near the Ig light chain (Ig/L). Ig heavy chain, Ig/H.

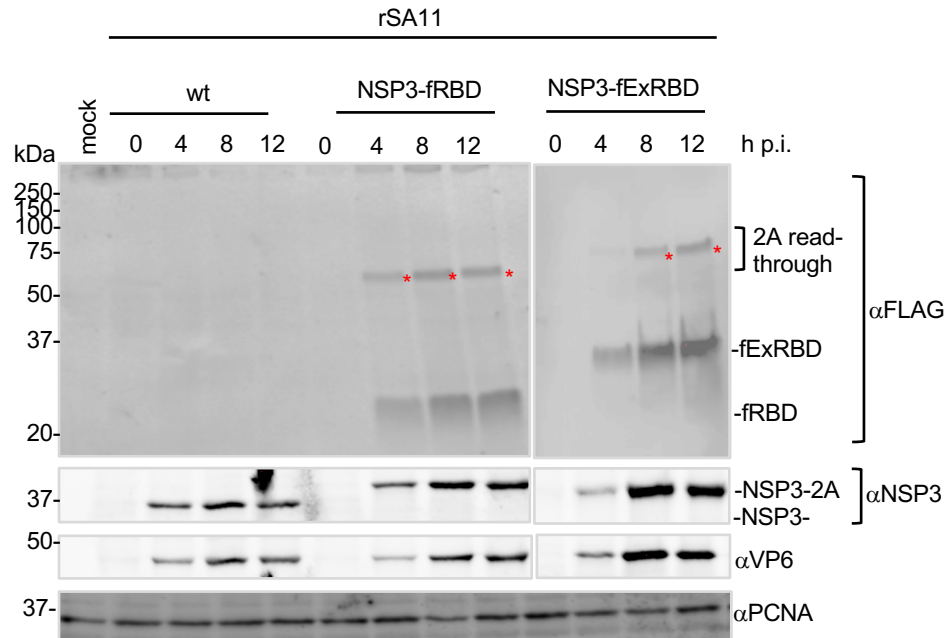


Figure 5. Production of RBD and ExRBD by rSA11 viruses during infection. MA104 cells were mock infected or infected with rSA11/wt, rSA11/NSP3-fRBD, or rSA11/NSP3-fExRBD (MOI of 5). Lysates were prepared from the cells at 0, 4, 8, or 12 h p.i. and analyzed by immunoblot assay using antibodies specific for FLAG, NSP3, VP6, and PCNA. Red asterisks identify 2A read-through products. Positions of molecular weight markers are indicated (kDa).

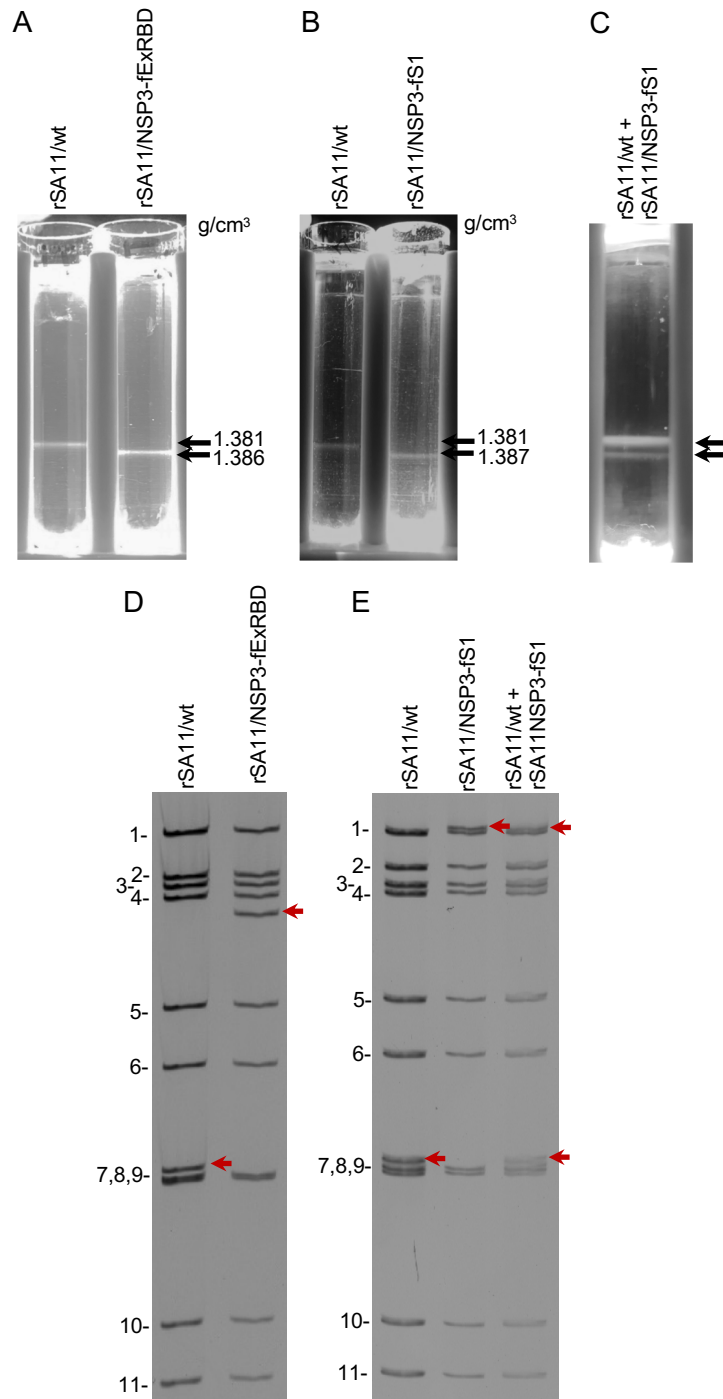


Figure 6. Impact of genome size on rotavirus particle density. MA104 cells were infected with rSA11/wt, rSA11/NSP3-fExRBD, or rSA11/NSP3-fS1 viruses at an MOI of 5. At 12 h p.i., the cells were recovered, lysed by treatment with non-ionic detergent, and treated with EDTA to convert rotavirus virions into DLPs. **(A, B)** DLPs were banded by centrifugation in CsCl gradients and their densities (g/cm^3) determined using a refractometer. **(C)** Lysates from rSA11/wt and rSA11/NSP3-fS1 infected cells were combined and their DLP components banded by centrifugation in a CsCl gradient. **(D,E)** Electrophoretic profile of the dsRNA genomes of DLPs recovered from CsCl gradients. Panel D RNAs derive from DLPs in panel A and panel E RNAs derive from DLPs in panel B and C. RNA segments of rSA11/wt are labeled 1 to 11. Positions of segment 7 RNAs are indicated with red arrows.

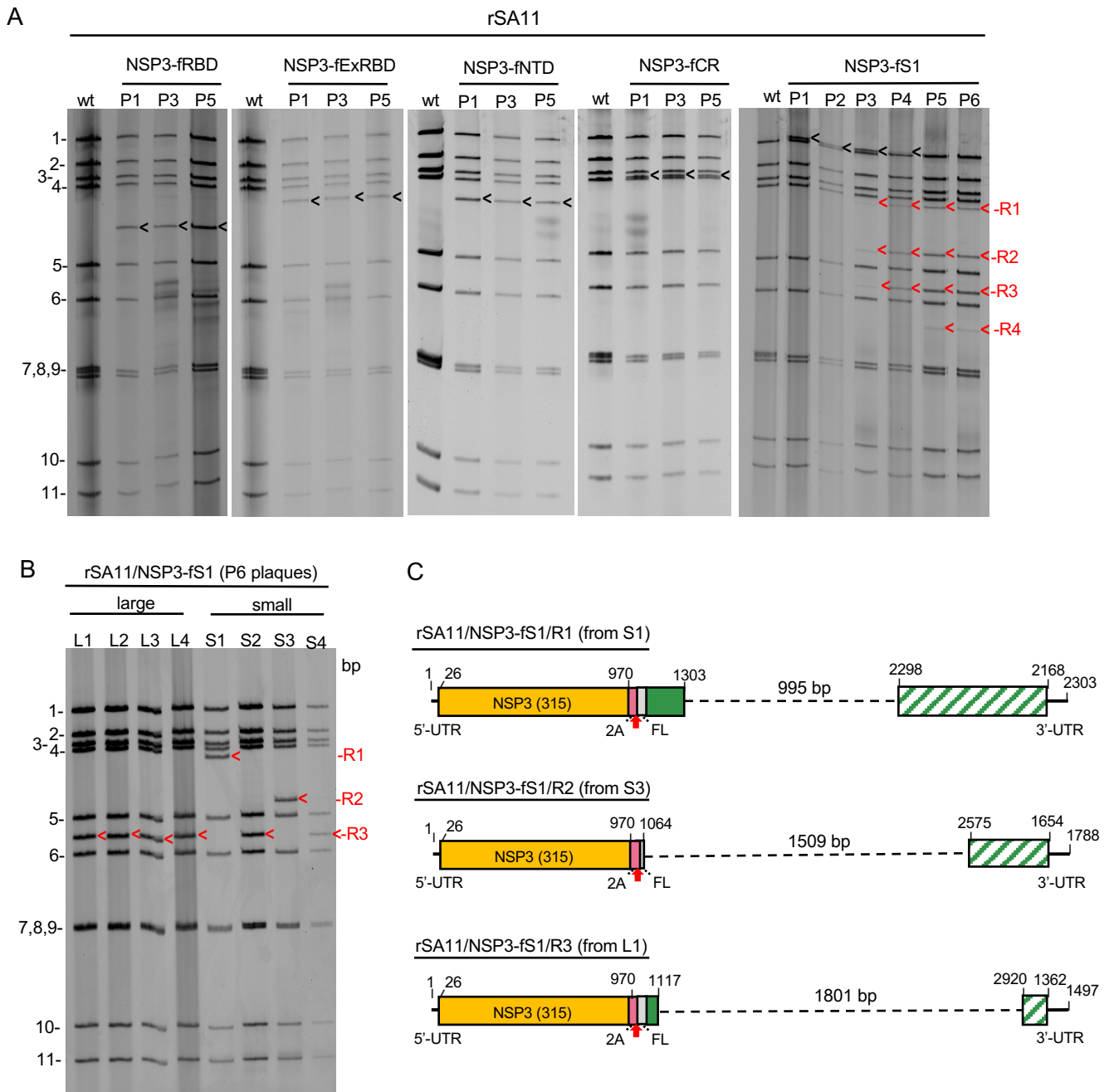


Figure 7. Genetic stability of rSA11 strains expressing SARS-CoV-2 S domains. rSA11 strains were serially passaged 5 to 6 times (P1 to P5 or P6) in MA104 cells. **(A)** Genomic RNAs were recovered from infected cell lysates and analyzed by gel electrophoresis. Positions of viral genome segments are labeled. Position of modified segment 7 (NSP3) dsRNAs introduced into rSA11 strains are denoted with black arrows. Genetic instability of the modified segment 7 (NSP3) dsRNA of rSA11/NSP3-fS1 yielded R1-R4 RNAs during serial passage. **(B)** Genomic RNAs prepared from large (L1-L4) and small (S1-S4) plaque isolates of P6 rSA11/NSP3-fS1. Segment 7 RNAs are identified as R1-R3, as in **(A)**. **(C)** Organization of R1-R3 sequences determined by sequencing of segment 7 RNAs of L1, S1, and S3 plaque isolates. Sequence deletions are indicated with dashed lines. Regions of the S1 ORF that are no longer encoded by the R1-R3 segment 7 RNAs are indicated by slashed green-white boxes.

Virus strain			Genome segment 7					NCBI accession #
Abbreviated name	Formal name*	Genome size/ increase over wt (bp)	RNA (bp)	Protein product				
				uncleaved (aa)	2A cleaved (aa)	uncleaved (kDa)	2A cleaved (kDa)	
rSA11/wt	RVA/Simian-lab/USA/SA11wt/2019/G3P[2]	18,559/0	1105	315	nd	36.4	nd	LC178572
rSA11/NSP3-INTD	RVA/Simian-lab/USA/SA11(NSP3-P2A-CoV2:fNTD)/2020/G3P[2]	19,537/978	2083	641	336 + 305	73.2	38.5 + 34.8	MW059024
rSA11/NSP3-fRBD	RVA/Simian-lab/USA/SA11(NSP3-P2A-CoV2:fRBD)/2020/G3P[2]	19,264/705	1810	550	336 + 214	62.7	38.5 + 24.3	MT655947
rSA11/NSP3-fExRBD	RVA/Simian-lab/USA/SA11(NSP3-P2A-CoV2:fExRBD)/2020/G3P[2]	19,564/1005	2110	650	336 + 314	74.7	38.5 + 35.2	MT655946
rSA11/NSP3-fCR	RVA/Simian-lab/USA/SA11(NSP3-P2A-CoV2:fCR)/2020/G3P[2]	19,798/1239	2344	728	336 + 392	81.4	38.5 + 42.9	MW059025
rSA11/NSP3-fS1	RVA/Simian-lab/USA/SA11(NSP3-P2A-CoV2:fS1)/2020/G3P[2]	20,752/2193	3298	1046	336 + 710	118.1	38.5 + 79.6	MW059026
rSA11/NSP3-fS1/R1	RVA/Simian-lab/USA/SA11(NSP3-P2A-CoV2:fS1/R1)/2020/G3P[2]	19,757/1198	2303	431	336 + 95	49.6	38.5 + 11.1	MW353715
rSA11/NSP3-fS1/R2	RVA/Simian-lab/USA/SA11(NSP3-P2A-CoV2:fS1/R2)/2020/G3P[2]	19,233/683	1789	367	336 + 31	42.1	38.5 + 3.7	MW353716
rSA11/NSP3-fS1/R3	RVA/Simian-lab/USA/SA11(NSP3-P2A-CoV2:fS1R3)/2020/G3P[2]	18,951/392	1497	410	336 + 74	47.2	38.5 + 8.8	MW353717

* Formal strain names were assigned according to Matthijnsens et al (45). nd: not determined, no 2A cleavage site present; wt: wild type

Table 2. Primers used to produce pT7/NSP3-2A-CoV2 plasmids.

Primer	Sequence
Vector_For	TGACCATTTTGATACATGTTGAACAATCAAATACAG
Vector_Rev	GCTAGCCTTGTCATCGTCATCCT
NTD_For	GATGACAAGGCTAGCTGTGTTAATCTTACAACCAGAACTCAATTACCCC
NTD_Rev	GTATCAAATGGTCAGTCAAGTGCACAGTCTACAGCATC
ExRBD_For	GATGACAAGGCTAGCGGAATCTATCAAACCTCTAACTTTAGAGTCCAACCA
ExRBD_Rev	GTATCAAATGGTCATGTTATAACACTGACACCACCAAAGAACA
RBD_For	GATGACAAGGCTAGCTTGTGCCCTTTTGGTGAAGTTT
RBD_Rev	GTATCAAATGGTCAAGTTGCTGGTGCATGTAGAAGT
CR_For	GATGACAAGGCTAGCTCTATTGCCATACCCACAAATTTACTATTAGTGT
CR_Rev	GTATCAAATGGTCAAGTTGTGAAGTTCTTTTCTTGTGCAGG
S1_For	GATGACAAGGCTAGCGTGTGTTGTTTTCTTGTTTTATTGCCACTAGTCT
S1_Rev	GTATCAAATGGTCAACGTGCCCGCCG